A study of instrumented indentation by finite element analysis

Minh-quy Le[a], Seock-sam Kim[b]

[a] Graduate School, School of Mechanical Engineering, Kyungpook National University, Daegu, South Korea

[b] School of Mechanical Engineering, Kyungpook National University, Daegu, South Korea

Abstract-Finite element computations were carried out to study the indentation by rigid cone with half-angle of 70.3^0 for 72 different combinations of elasto-plastic properties that cover the wide range of mechanical parameters of common engineering solid materials. The dimensional analysis and representative strain concept were used in the analysis. It was shown that for the same representative strain value, the loading curvature C can be formulated under two different forms, which are based on two alternative dimensionless functions. The present study's one is simpler than the other previously found by other authors using the similar approach. For a wide range of material's parameters, the hardness-modulus ratio should be a parabolic function of σ_r/E, rather than a power law function earlier proposed.

Keywords: instrumented indentation, finite element.

1. Introduction

Indentations have been used since longtime to determine the material's hardness [1]. Actually, Instrumented indentation techniques have been developed extensively to characterize materials [2]. The hardness and modulus can be determined directly from the instrumented indentation data [3]. Associating to finite element computations, these techniques can be extended to extract the mechanical properties of the indented materials such as yield strength and strain hardening exponent [4-9,11,14].

Jayaraman et al. [4], using the hardness values related to different angle conical indenters, gave a method for determining the non-linear part of stress–strain curve. Giannakopoulos and Suresh [8] have used two parts of the loading and unloading Vickers indentation curve for yield stress and hardening exponent determination. They determine yield stress and stress at 0.29 plastic strain so the hardening exponent can be determined from these values. But in another paper [9], the authors specified that their approach could not distinguish two different materials, which have the same yield stress Y and the same $\sigma_{0.29}$ stress obtained for a plastic strain equal to 0.29. The use of a Vickers indenter leads to the load–displacement $P=Ch^2$ relation (Fig. 1), which is based on the determination of only one parameter C and cannot lead to the uniqueness. This was indicated by [10]. Dao et al. [11] proposed a method to estimate the mechanical properties from loading curvature C, the slope of the load-displacement curve at initial unloading and the residual indentation depth-to-maximum indentation depth ratio. This work has been extended by [6] for different sharp indenters.

Therefore, in order to extract the material's mechanical properties from the indentation load-displacement curve, the relationships between the material's mechanical properties and indentation parameters such as loading curvature *C*, hardness, residual indentation depth- maximum indentation depth ratio ...have to be formulated. The aim of this work is to present a short study on the loading curvature C and hardness-modulus ratio based on the dimensional analysis and representative strain concept. The results are useful for the stress–strain curve determination from instrumented indentation tests, which will be presented in another paper.

2. Theoretical backgrounds and finite element model

2.1. *Material's description*

Plastic behavior of many engineering solid materials can be modeled by a power law description, as shown schematically in Fig. 2. A simple elasto-plastic, true stress–true strain behavior is assumed to be

$$\begin{aligned} \sigma &= E.\varepsilon, \quad (\sigma \le Y) \\ \sigma &= K.\varepsilon^{n}, \quad (\sigma \ge Y) \end{aligned} \qquad (1)$$

where E is the Young's modulus, K a strength coefficient, n the strain hardening exponent, Y the initial yield stress and ε_y the corresponding yield strain, such that

$$Y = E\varepsilon_y = K\varepsilon_y^{n} \qquad (2)$$

Here the yield stress Y is defined at zero offset strain. The total strain, ε, consists of elastic strain ε_e and plastic strain ε_p:

$$\varepsilon = \varepsilon_e + \varepsilon_p \quad (3)$$

The representative strain ε_r, defined by Dao et al. [11], corresponds to the strain accumulated beyond the yield point ε_y.

$$\varepsilon = \varepsilon_y + \varepsilon_r \quad (4)$$

With (2) and (4), when $\sigma > Y$, equation (1) becomes

$$\sigma = Y\left(1 + \varepsilon_r \frac{E}{Y}\right)^{n} \qquad (5)$$

To complete the material constitutive description, Poisson's ratio is designated as ν, and the incremental theory of plasticity with von Mises effective stress (J_2 flow theory) is assumed. Therefore, a material's elasto-plastic behavior is fully determined by one of three parameter sets (E, ν, Y and n), (E, ν, σ_r and n) or (E, ν, Y and σ_r).

2.2. Review of dimensional analysis

The loading part of an instrumented indentation can be expressed as

$P=Ch^2$ (6)

where P is the indentation load, h is the penetration depth measured from surface, and C is a constant depending on the geometry of the indenter tip and material properties.

Many authors used dimensional analysis [11-14] to propose a number of dimensionless universal functions. Some of them are briefly summarized here for C.

For a sharp indenter (conical, Berkovich or Vickers, with fixed indenter shape and tip angle) indenting normally into a power law elasto-plastic solid, the load P can be written as

$P=P(h,E,\nu,E_i,\nu_i,Y,n)$, (7)

where E_i is Young's modulus of the indenter, and ν_i is its Poisson's ratio. This functionality is often simplified by combining elasticity effects of an elastic indenter and an elasto-plastic solid as

$P=P(h,E^*,Y,n)$, (8)

where

$$\frac{1}{E^*}=\frac{1-\nu}{E}+\frac{1-\nu_i^2}{E_i} \quad (9)$$

For a rigid indenter, we have $E=E^*$ since $E_i=\infty$. In the present paper, the use of E and E^* are consistent.

Since a material's elasto-plastic behavior is fully described by one of three parameter sets (E, ν, Y and n), (E, ν, σ_r and n) or (E, ν, Y and σ_r), alternatively, equation (8) can be written as

$P=P(h,E^*,\sigma_r,n)$ (10)

Or $P=P(h,E^*,Y,\sigma_r)$ (11)

Applying the Π theorem in dimensional analysis, equation (9) becomes

$$P=\sigma_r h^2 \Pi_1\left(\frac{E^*}{\sigma_r},n\right) \quad (12a)$$

and thus

$$C=\frac{P}{h^2}=\sigma_r \Pi_1\left(\frac{E^*}{\sigma_r},n\right) \quad (12b)$$

where Π_1 is a dimensionless function. Similarly, applying the Π theorem to equation (10), loading curvature C may alternatively be expressed as

$$C=\frac{P}{h^2}=Y\Pi_1^A\left(\frac{E^*}{Y},\frac{\sigma_r}{Y}\right) \quad (13a)$$

$$\text{or } C=\frac{P}{h^2}=\sigma_r \Pi_1^B\left(\frac{E^*}{\sigma_r},\frac{Y}{\sigma_r}\right) \quad (13b)$$

By similar way, the hardness-modulus ratio can then be determined for the case of rigid indenter as follow

$$\frac{H}{E}=\frac{\sigma_r}{E}\Pi_3\left(\frac{\sigma_r}{E},n\right) \quad (14)$$

2.3. Finite element model

Elastic-plastic indentation was simulated using the axisymmetric capacities of the MARC finite element code. Since the projected contact area for a conical indenter, a Berkovich indenter and a Vickers indenter are $A=\pi h^2\tan^2\theta$; $A=24.56h^2$; and $A=24.50h^2$, respectively; the indenter was modeled as a rigid cone with a half-included angle of $\theta=70.3^0$. This angle gives the same area-to-depth ratio as the Berkovich or Vickers indenter, which are commonly used in instrumented-indentation experiments.

The specimen was modeled as a large cylinder 100μm in height and 100μm in radius represented by 3400 four-node axisymmetric elements (Fig. 3). These dimensions were found to be large enough to approximate a semi-infinite half-space for indentations with maximum depth of $\leq$0.5 μm, which are considered in the present work. This was evidenced by an insensitivity of calculated results to further increase in specimen size.

Elements were finest in the central contact area and became coarser outwards. The smallest element size was 7nm, which enables an accurate determination of the real impression size. Roller boundary conditions were applied along the centerline and bottom. Outside surfaces were taken as free surfaces. The interaction between the diamond indenter and specimen was modeled by contact elements with no friction.

A large number of 72 different combinations of elasto-plastic properties with n ranging from 0 to 0.5 and Y/E ranging from 0.001 to 0.022 were used in the computations. This wide range of parameters covers mostly engineering solid materials. The material's mechanical properties used in the computations are given in the table 1.

3. Results and Discussion

3.1 The loading curvature C

The relation in equation (6) has been demonstrated by numerical simulation for elastic–plastic materials [12,13,15-19]. The constant C in equation (6) can be found in [15-22], based on different approaches.

The loading curvature C was formulated by [15,20-22] as

$$C = M_1\sigma_{0.29}\left(1+\frac{Y}{\sigma_{0.29}}\right)\left[M_2+\ln\left(\frac{E^*}{Y}\right)\right] \quad (15)$$

where M_1 and M_2 are computationally derived constants which depend on indenter geometry; and $\sigma_{0.29}$ is the flow stress at plastic strain σ_p=0.29.

Recently, Dao et al. [11] using dimensional analysis and finite element computation proposed the formulae of C as follow:

$$\Pi = \frac{C}{\sigma_{0.033}} = -1.131\left[\ln\left(\frac{E^*}{\sigma_{0.033}}\right)\right]^3 + 13.635\left[\ln\left(\frac{E^*}{\sigma_{0.033}}\right)\right]^2 - 30.594\left[\ln\left(\frac{E^*}{\sigma_{0.033}}\right)\right] + 29.267 \quad (16)$$

where $\sigma_{0.033}$ is the flow stress at ε_r=0.033.

It is interesting to note that, after rewriting $\sigma_{0.29}(1+Y/\sigma_{0.29})$ as $Y(1+\sigma_{0.29}/Y)$ in equation (15), this equation is consistent with equation (13a).

For this reason, we propose to use the dimensionless function $C/(Y+\sigma_r)$ instead of C/σ_r as cited by [11], and plot this function against ln(E/Y). The purpose is to find if the representative strain exists for the formulation of the parameter C under the form of (15).

Figure 4 presents the evolution of $C/(Y+\sigma_r)$ versus ln(E/Y) for three different values of ε_r (ε_r=0.002, 0.033 and 0.29). It is interesting to find that the representative strain in the present case is consistent to ε_r=0.033, which was found by [11]. Figure 4 shows that for ε_r<0.033, $C/(Y+\sigma_r)$ increases while increasing n and for ε_r>0.033, $C/(Y+\sigma_r)$ decreases while increasing n.

We should emphasize here the representative strain depends on the chosen dimensionless function. In the present study, the dimensionless function for C is $C/(Y+\sigma_r)$ versus E^*/Y. In [11], the dimensionless function for C is C/σ_r versus E^*/σ_r. However, the representative strains in two cases are consistent. The reason for this is that the two dimensionless functions used are equation (12a) and (11b), which are in the alternative form.

For ε_r=0.033, the dimensionless function $C/(Y+\sigma_r)$ can be interpolated by a linear function of $\ln(E/Y)$ with the correlation coefficient R^2=0.9971.

$$\frac{C}{(Y+\sigma_{0.033})} = N_1\left[N_2 + \ln\left(\frac{E^*}{Y}\right)\right] \quad (17)$$

where N_1=13.36 & N_2 =-25.52

This description of C is more simple than (16), in which $C/\sigma_{0.033}$ is expressed by a of third order polynomial of $\ln(E^*/Y)$.

The parameter C normalized by E* is plotted in Fig. 4d for equation (16) and (17). In general, these to curve are consistent.

3.2 The hardness

The equation (14) is used to consider the evolution of the dimensionless function H/E versus σ_r /E for various values of n ranging from 0 to 0.5 as presented in Fig. 5 with three different values of ε_r (ε_r=0; 0.063 and 0.29).

The representative strain ε_r=0.063 is found in this case. Figure 5 shows that for ε_r<0.063, H/E increases while increasing n and for ε_r>0.063, H/E decreases while increasing n.

When ε_r =0, 063, all of data points with n ranging from 0 to 0.5 can be well fitted by a second order polynomial with the correlation coefficient R^2=0.9996 as follow:

$$\frac{H}{E} = A_1\left(\frac{\sigma_r}{E}\right)^2 + A_2\left(\frac{\sigma_r}{E}\right) \quad (18)$$

where $\sigma_r=\sigma_{0.063}$, A_1=-16.24 and A_2=2.83.

S. Jayaraman et al. [4] supposed that the characteristic plastic strain ε_p is related to the hardness by a power law function (19) similar to the simple Ramberg–Osgood equation (20)

$$\varepsilon_p = L'(H/E)^{N'} \quad (19)$$

$$\varepsilon_p = L(\sigma_r/E)^N \quad (20)$$

Based on these two equations, the hardness-flow stress and characteristic plastic strain-cone angle correlations, for conical indenters were obtained from 12 different stress-strain curves, in which the strain hardening exponent n are 0.1,0.2 and 0.3, using the finite element method as follow:

$$\frac{H}{E} = A\left(\frac{\sigma}{E}\right)^{B} \tag{21}$$

where $\sigma=\sigma_{0.07}$, flow stress at plastic strain $\varepsilon_p=0.07$; A=1.17 and B=0.92.

This result was shown by [3] to lie between that predicted by the slip line field theory and the spherical cavity expansion model.

In the present study, it is found that with ε_r =0, 063, all of data points with n ranging from 0 to 0.5 can be also fitted by a power function under the form (21), however this function cannot be well consistent with certain value of H/E as shown in Fig. 5c. Fig. 6 shows the comparison of the present result and [3].

4. Conclusion

Large deformation finite element computations were carried out for 72 different combinations of elasto-plastic properties that cover the wide range of mechanical parameters of common engineering solid materials. This study focused mainly on the loading curvature C and hardness-modulus ratio of the indented material based on the dimensional analysis and representative strain concept. The main results of the present study are summarized as follows:

1. It is shown that for the same representative strain value, the loading curvature C can be formulated under two different forms, which are based on two alternative dimensionless functions. The present study's one is simpler than the other previously found by Dao et al. [11] using the similar approach.
2. For a wide range of material's parameters, the hardness-modulus ratio should be a parabolic function of σ_r/E, rather than a power law function earlier proposed.
3. The results are useful for predicting the indentation loading-displacement curve and hardness of material when the mechanical properties of the material are known; and for the stress–strain curve determination from instrumented indentation tests, which will be presented in another paper.

References

1. D. Tabor, The Hardness of Metal. , Clarendon Press, Oxford (1951).
2. A.C. Fischer-Cripps, Nanoindentation, Springer-Verlag, New York, 2002.
3. Oliver, W.C.; Pharr, G.M, *Journal of Materials Research*, 7, 6, (1992), pp. 564
4. S. Jayaraman, G.T. Hahn, W.C. Oliver, C.A. Rubin and P.C. Bastias , *Int. J. Solid Struct.* 35,

5-6 (1998), pp. 365–381.

5. M. Futakawa, T. Wakui, Y. Tanabe and I. Ioka, *Journal of Materials Research*. 16, 8, (2001), pp. 2283.
6. J. L. Bucaille, S. Stauss, E. Felder and J. Michler, *Acta Materialia*, 51, 6, (2003), 1663-1678.
7. S. Stauss, P. Schwaller, J. -L. Bucaille, R. Rabe, L. Rohr, J. Michler and E. Blank, *Microelectronic Engineering*, 67-68, (2003), 818-825.
8. A.E. Giannakopoulos and S. Suresh, *Scr. Mater.* 40, 10 (1999), pp. 1191–1198.
9. T.A. Venkatesh, K.J. Vliet, A.E. Giannakopoulos and S. Suresh, *Scr. Mater.* 42, 9 (2000), pp. 833–836.
10. Y.T. Cheng and C.T. Cheng, *J. Mater. Res.* 14 (1999), pp. 3493–3496
11. M. Dao, N. Chollacoop, K.J. Van Vliet, T.A. Venkatesh and S. Suresh, *Acta Mater.* 49 (2001), p. 3899-3918.
12. Y.T. Cheng and C.M. Cheng. *J. Appl. Phys.* **84** (1998), p. 1284.
13. Y.T. Cheng and C.M. Cheng. *Appl. Phys. Lett.* **73** (1998), p. 614.
14. K. Tunvisut, N.P. O'Dowd and E.P. Busso. *Int. J. Solids Struct.* **38** (2001), p. 335.
15. A.E. Giannkopoulos, P.-L. Larsson and R. Vestergaard. *Int. J. Solids Struct.* **31** 19 (1994), p. 2679.
16. P.-L. Larsson, A.E. Giannakopoulos, E. Söderlund, D.J. Rowcliffe and R. Vestergaard. *Int. J. Solids Struct.* **33** 2 (1996), p. 221.
17. A.E. Giannakopoulos and P.-L. Larsson. *Mech. Mater.* **25** (1997), p. 1.
18. B.J. Briscoe, K.S. Sebastian and M.J. Adams. *J. Phys. D: Appl. Phys.* **27** (1994), p. 1156.
19. G.G. Bilodeau. *J. Appl. Mech.* **59** 9 (1992), p. 519
20. A.E. Giannakopoulos and S. Suresh. *Scripta mater.* **40** (1999), p. 1191.
21. T.A. Venkatesh, K.J. Van Vliet, A.E. Giannakopoulos and S. Suresh. *Scripta mater.* **42** (2000), p. 833.
22. P.-L. Larsson, A.E. Giannakopoulos, E. Soderlund, D.J. Rowcliffe and R. Vestergaard. *Int. J. Solids Struct.* **33** (1996), p. 221.

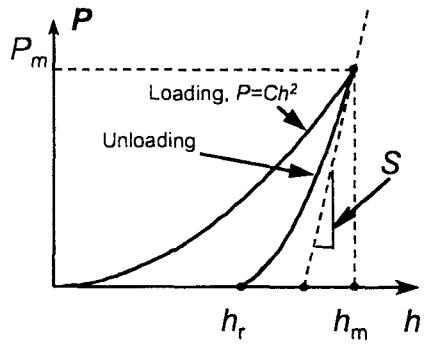

Fig. 1. Schematic illustration of the indentation load-displacement curve of an elasto-plastic material.

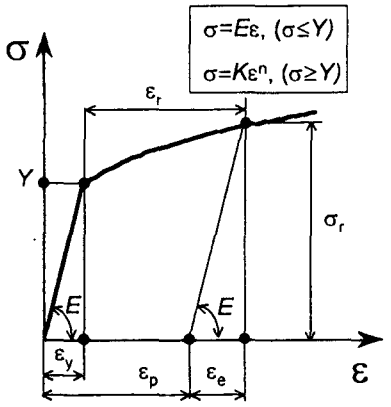

Fig.2. The power law elasto-plastic stress-strain behavior.

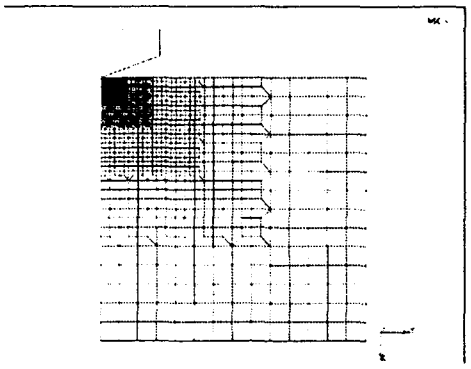

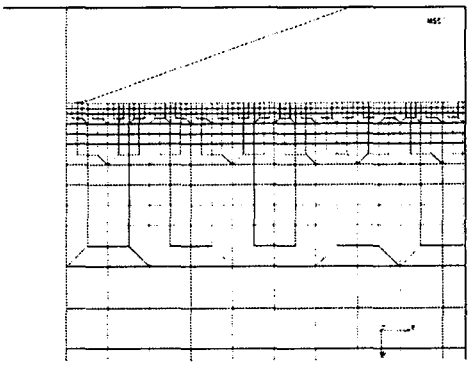

Fig.3. Finite element meshing of half-space and zoom of the contact zone

Table 1. The material's mechanical properties used in the computations

E, GPa	140	140	140	200	200	310	140	200	200	140	310	310
Y/E	0.001	0.002	0.004	0.006	0.008	0.01	0.012	0.014	0.016	0.018	0.02	0.022

Strain hardening exponent, n=0, 0.1, 0.2, 0.3, 0.4, 0.5;

Poisson's ratio, ν, was fixed at 0.25.

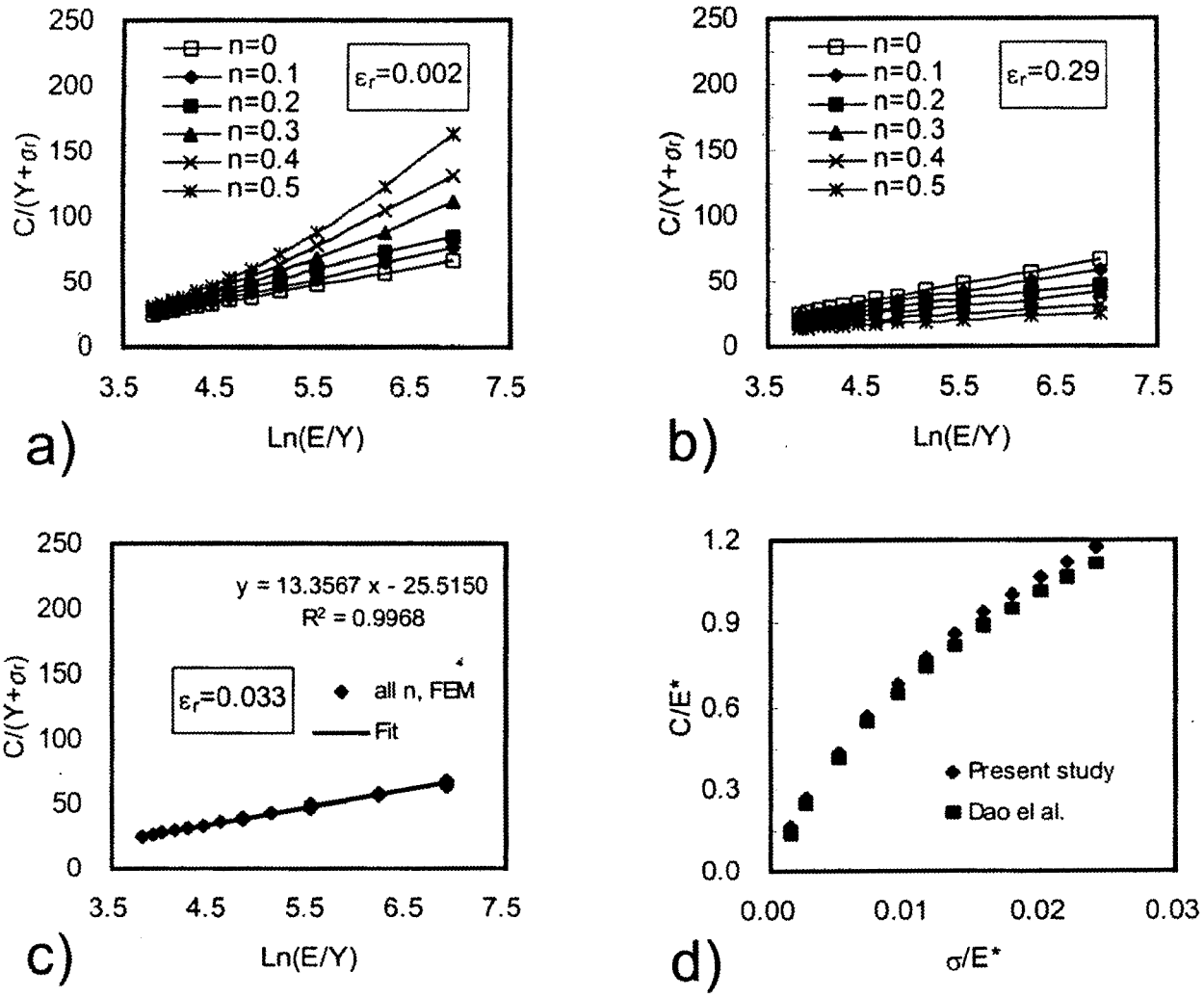

Fig.4. a, b, c) Evolution of dimensionless function C/(Y+ σ_r) versus ln(E/Y) using three different values of ε_r with respect to n=0, 0.1, 0.2...0.5; and d) Comparison between the present result and Dao et al. [11]

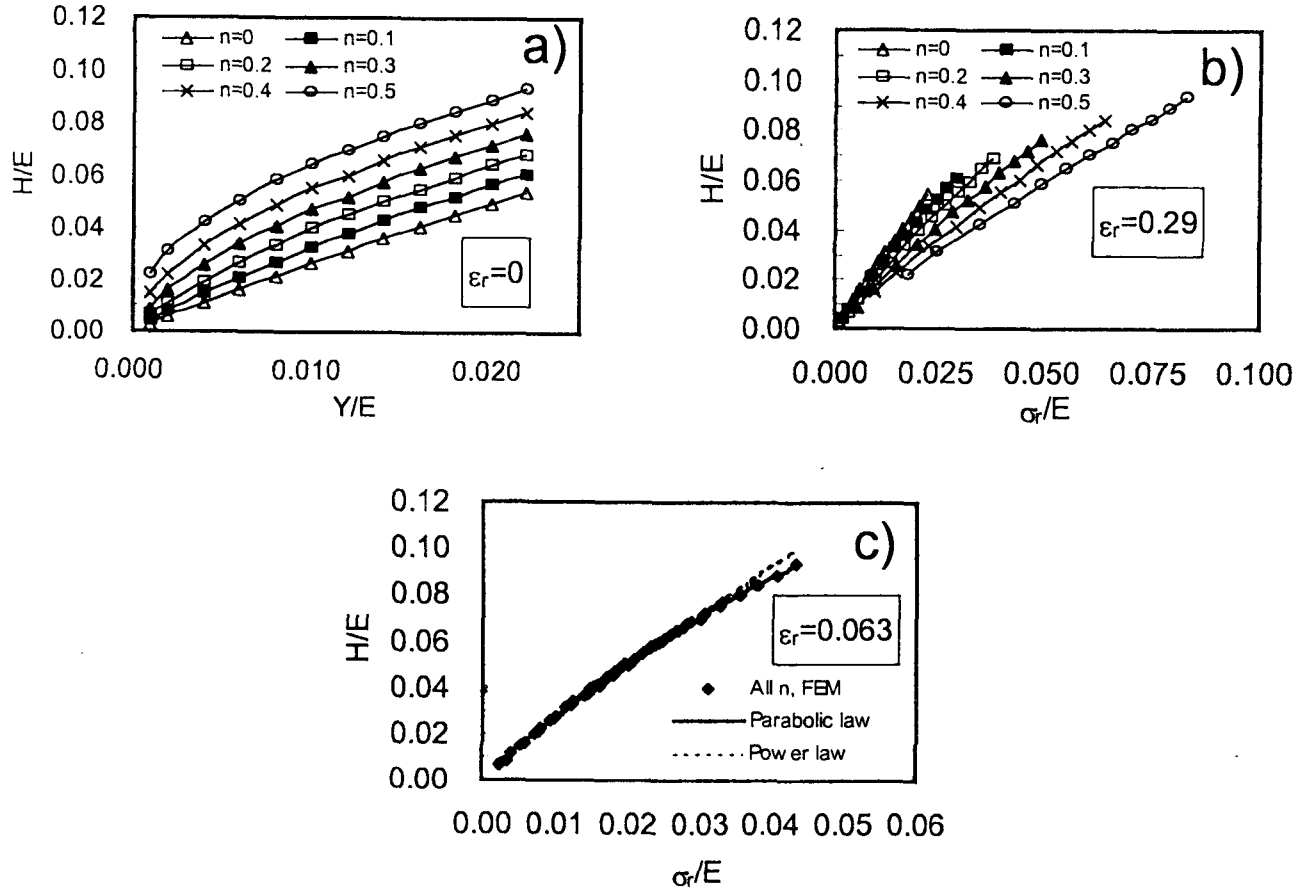

Fig.5. Evolution of the hardness-modulus ratio versus σ_r/E using three different values of ε_r with respect to n=0, 0.1, 0.2...0.5.

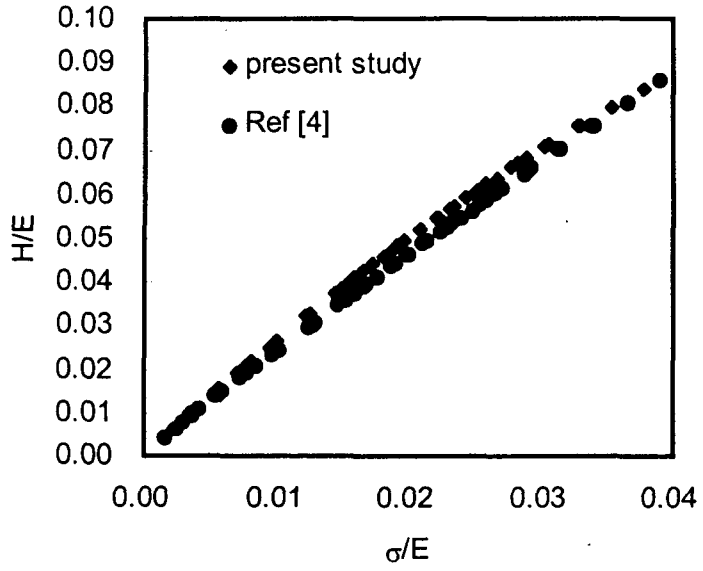

Fig.6. Evolution of the hardness-modulus ratio versus σ/E

논 문 발 표

Session III(B) 윤활공학 및 트라이볼로지 설계